Long-Period Fiber Grating based on Side-Polished Optical Fiber and Its Sensing Application

Hou-Chang Li（李厚昶）, Juan Liu (刘娟), Xing-Dao He（何兴道）, Jinhui Yuan (苑金辉), Qiang Wu* and Bin Liu*（刘彬）

Abstract—A novel side-polished long-period fiber grating (LPFG) sensor was proposed and experimentally validated. Side-polished can provide a stronger evanescent field than traditional grating and bring superior sensitivity. The greater the side-polished depth, the higher the refractive index (RI) sensitivity. When d = 44 μm, the refractive index sensitivity reached 466.85 nm/RIU in the range of 1.3330 - 1.3580, which is four-fold higher than LPFG prepared by electric-arc discharge (EAD) method. A graphene oxide (GO) nano-film is coated on the LPFG to make it realize high sensitivity relative humidity (RH) sensing. Humidity sensitivity reached -0.193 nm/%RH in the range of 40 - 80% RH. In addition, side-polished breaks the symmetry of the distribution of the cross-sectional light field, which determines the ability to achieve vector curvature measurement. It shows good sensing performance in the same/opposite bending direction as the side polished surface. When the input light polarization is 90°, the average sensitivity reaches 5.03 and -5.9 nm/m^{-1} in the range of 0 - 19.67 m^{-1}, respectively. This strongly indicates that the fabricated sensors show high sensitivity, low-cost materials, and robust performance and break the limitations of the EDA method to prepare gratings, which have good application potential for biomedicine and the field of construction.

Keywords: Long-period fiber grating, side-polished, relative humidity sensing, vector curvature sensing.

I. INTRODUCTION

Fiber grating is an optical fiber microstructure formed by periodically modulating the refractive index (RI) of the optical fiber [1,2]. It has the characteristics of small size, good wavelength selectivity, corrosion resistance, and strong anti-interference performance, and is widely used in various sensor designs [3-7]. At present, it has been maturely applied in aerospace, medicine, geological survey, power system, and other fields.

The period of long-period fiber grating (LPFG) is usually tens to hundreds of microns, so its requirements for fabrication equipment are much lower than that of fiber Bragg grating (FBG) [8]. Currently commonly used writing methods include ultraviolet or femtosecond laser irradiation fabrication [9,10], mechanical induction [11], chemical etching [12], ion beam implantation [13], and thermal application generation through spatial periodicity [14-16]. Among them, the electric-arc discharge (EAD) method is to melt and deform the optical fiber through the periodic discharge of the electrode, so that the RI of the optical fiber is periodically modulated to form a fiber grating. The preparation mechanism of this method is similar to that of a CO_2 laser, and gratings can be directly prepared on any type of optical fiber, without the need for the optical fiber to have photosensitivity or other hydrogen-carrying sensitization treatments. It has the advantages of simple manufacture, low cost, and good stability. And the amplitude of the current and the discharge time can be freely adjusted to control the amplitude of the RI modulation. However, the surrounding refractive index (SRI) sensitivity of LPFG is usually lower until further optimization is applied [17]. Thus, LPFGs need further optimization for better performance. To overcome this limitation, modified methods have been proposed. For example, in 2017, Du *et al.* [18] fabricated an LPFG sensor using EAD technology. The RI sensitivity was optimized by etching the cladding with a hydrofluoric acid solution, and the sensitivity reached 214 nm/RIU in the range of 1.3333 - 1.3931. The drawback of this method is that the use of hydrofluoric acid (HF) will weaken the mechanical strength of the sensor and HF are hazardous, corrosive, and toxic. In 2020, Luo *et al.* [19] fabricated an LPFG on a thin-clad fiber (TCF) using EAD technology, and the sensitivity could reach -51.72 nm/RIU in the RI range of 1.3406 - 1.4096. However, limited ability to improve RI sensitivity by TCF. In 2014, L. Coelho *et al.* [20] studied a new type of optical fiber RI sensor based on an LPFG coated with a titanium dioxide (TiO_2) film, and the average sensitivity obtained in the range of 1.444~1.456 was 5250 nm/RIU. However, this method has high costs (including high consumables and expensive coating equipment). In 2021, Y. Zhou *et al.* [21] studied the sensing properties of double-clad fiber (DCF) long-period fiber grating (LPFG) to the SRI. The numerical simulation results show that the SRI sensitivity is

This work was supported by the National Natural Science Foundation of China (NSFC) (11864025, 62175097, 62065013, and 62163029); Natural Science Foundation of Jiangxi Province (20212BAB202024 and 20192ACB20031). (Correspondence authors: Bin Liu and Qiang Wu)

Hou-Chang Li, Juan Liu, Xing-Dao He, Qiang Wu and Bin Liu are with Key Laboratory of Opto-Electronic Information Science and Technology of Jiangxi Province, Nanchang Hangkong University, Nanchang 330063, China (e-mail: lihouchang104@163.com; 18042@nchu.edu.cn; hxd@nchu.edu.cn; qiang.wu@northumbria.ac.uk; liubin@nchu.edu.cn). Qiang Wu is also with Faculty of Engineering and Environment, Northumbria University, Newcastle Upon Tyne NE1 8ST, UK.

Jinhui Yuan is with the Research Center for Convergence Networks and Ubiquitous Services, University of Science & Technology Beijing, Beijing 100083, China. (e-mail: yuanjinhui81@163.com)

greatly improved, reaching 3484.0 nm/RIU in the range of SRI 1.33-1.37. Apart from the above, the arc discharge method has certain limitations compared to the CO_2 laser irradiation method. The CO_2 laser irradiation method can achieve LPFGs with arbitrary patterns [22], but the LPFGs fabricated by EAD technology have structural symmetry, which makes their application in curvature sensing generally independent of orientation. Similarly, researchers have also proposed some methods. For example, in 2018, Yang et al. fabricated an LPFG in Dual Side Hole Fiber (DSHF) by using the automatic EAD technique. The presence of DSHF makes the cladding modes, regardless of the polarization state, concentrated in the region perpendicular to the connection of the two holes, which makes DSHF-based LPFG suitable for biaxial bending measurements [23]. However, this type of method is limited by the type of optical fiber and does not have universal applicability. To further expand the application range of LPFG, it is necessary to try to improve the grating fabrication based on the EAD technology, improve the interaction between the evanescent wave and the surrounding medium, and optimize the performance of the fiber grating.

As a result, we propose and fabricate a novel side-polished LPFG and conducted a comprehensive study of its sensors. The introduction of side-polished will not only increase the evanescent field of the LPFG and thus improve RI sensitivity, but also break the symmetry of the intensity distribution of the cross-section light field, which makes it to be more suitable for sensing in different bending directions. By functionalization of a thin layer of GO layer on the side-polished region of the fiber, the sensor can measure RH with high sensitivity. Therefore, based on further optimization, it is expected to greatly improve the performance of LPFG.

II. Principle

The schematic diagram of side-polished LPFG is presented in Fig. 1(a). To analyze the fabricating parameters of the side-polished LPFG, the structural characterization of the samples was performed using an electron microscope (AO-UV200), as shown in Figs. 1(b)-(d).

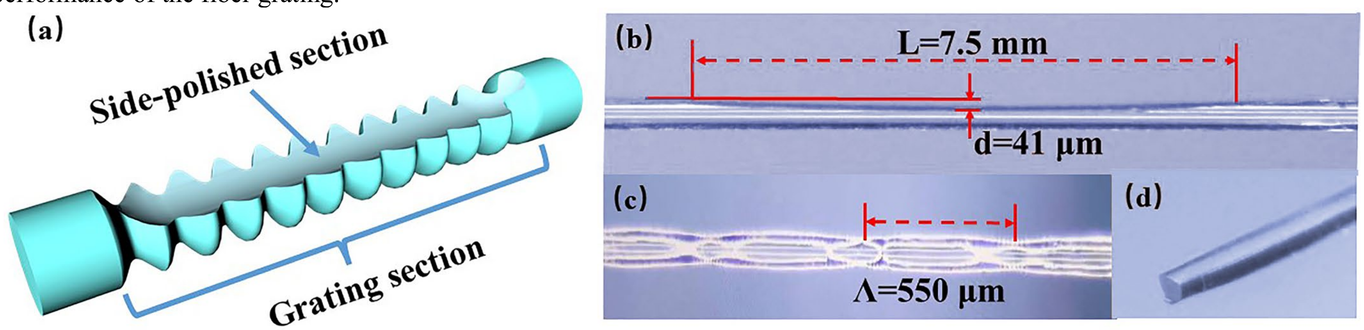

Fig. 1. (a) Schematic diagram of the side-polished LPFG; (b) optical microscope image of the side-polished fiber; (c) optical image microscope of the LPFG; (d) optical microscope image of the end-face of the side-polished fiber.

The resonant wavelength is defined by the phase-matching condition [24]:

$$\lambda_{res}^{n} = \left(n_{eff,co} - n_{eff,cl}^{n} \right) \Lambda \tag{1}$$

Where $n_{\mathrm{eff},\ co}$ and $n_{\mathrm{eff},\ cl}^{n}$ are the effective RI of the core fundamental mode and the *n*th order cladding modes, and Λ is the grating period. The essence of LPFG is that the light generated from the core mode is coupled to the cladding mode whose wavelength satisfies the phase matching condition.

Once the light is coupled into the cladding mode, it immediately attenuates due to scattering losses, thus leaving a lossy band in the core mode observed at the output. When light travels in the cladding mode, it experiences high losses, which provide an attenuation band at the resonant wavelength in the transmission spectrum. The minimum transmission in the attenuation band is expressed by the formula:

$$T_m = 1 - sin^2(\kappa_m L) \tag{2}$$

where κ_m is the coupling coefficient of the mth cladding mode, and L is the length of the LPFG. The coupling coefficient is determined by the integral overlap of the core and cladding modes and the periodic modulation amplitude of the mode propagation constants. The number of cladding modes depends on the radius of the cladding.

III. Manufacture of sensor

An autonomous built system is used to fabricate the polished surface shown in Fig. 2(a). The optical fiber is fixed by two three-dimensional translation stages, and the polished unit is a motor of high rotating speed. The maximum speed of the motor is 12,000 revolutions per minute (RPM), and to ensure the mechanical stability of the fiber during side throwing, the rotational speed is limited to no more than 5000 RPM/min. A piece of sandpaper is firmly wound around the exposed shaft of the DC motor, about 3 cm in diameter, and used as a polished machine [25]. During polished, use 400, 600, and 800 grit sandpaper once each, and finish with 800 grit paper (minimize topographic effects by fine polished the surface of the sample). The side-polished depth is proportional to time, and the side-polished length is controlled by adjusting the angle between the fiber and the grinding wheel through a three-dimensional translation stage. Then, use the EAD (FSM-80c, Fujikura) to high-temperature fused-taper (the discharge time and power are 2000 ms and 12.7 mA respectively) on the polished area and pulled a Λ distance by attaching the other end with a weight (Fig. 2(b)). During discharge, the polished side is facing straight up, and the electrodes are discharged from the left and right sides perpendicular to the fiber. Spectral changes were detected by a light source (BBS, ASE-C-30-B) and a spectrometer (OSA, YOKOG AWA AQ6370D).

The experimental results of the spectrum evolution of the side-polished LPFG with a pitch of 550 μm and the number of cycles increased from 0 to 11 are shown in Fig. 2 (c). Where there is a resonance peak at 1510 nm, and the resonance intensity is about 10 - 15 dB when the number of periods is 15. The main features of this method are its simple production and lower cost. Therefore, with this stability setting, high-quality and repeatable gratings can be easily manufactured.

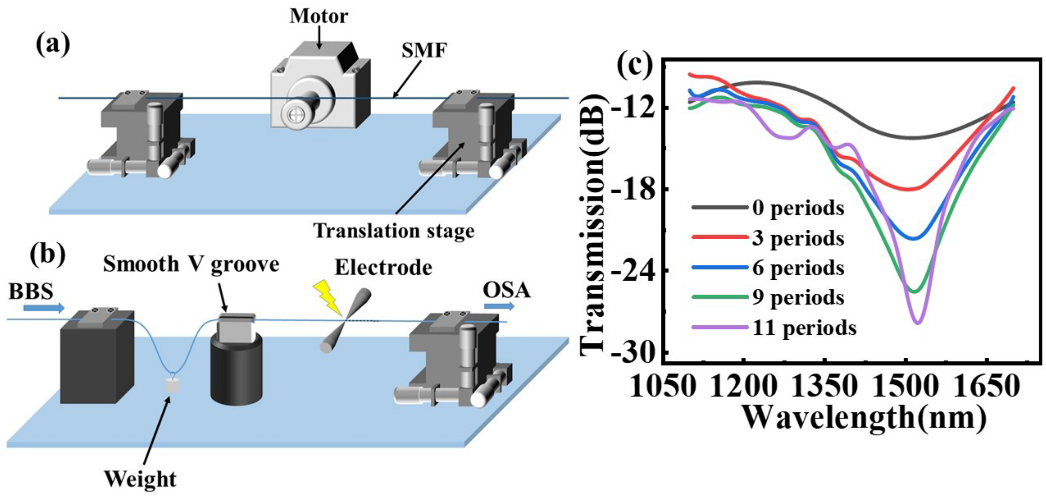

Fig. 2. (a) Side-polished fiber production platform; (b) LPFG production platform; (c) LPFG transmission spectrum change.

IV. RI SENSING PERFORMANCE

When the surrounding RI of the side-polished LPFG changes, the effective RI of the cladding mode of the fiber will change, resulting in the change in the phase-matching wavelength of the LPFG [26]:

$$\frac{d\lambda}{dn_{medium}} = \frac{d\lambda}{dn^{n}_{eff,cl}} \frac{dn^{n}_{eff,cl}}{dn_{medium}} \tag{3}$$

Where dn_{medium} is effective RI of the medium. The term $dn^{n}_{eff,cl}/dn_{medium}$ is different for different cladding modes. The experimental setup for investigating the RI measurement capability of the fabricated side-polished LPFGs is shown in Fig. 3. The liquid with different RI (dimethyl sulfoxide mix with water, which has been calibrated using an Abbe refractometer) was dropped into the U-shape groove container, and the change in the transmission signal from side-polished LPFGs was detected by OSA. Rinse the sensor with deionized water at least three times and air dry before each RI solution change. Before the measurement, the sensor was calibrated to assure that the results were both accurate and reliable. The entire experimental process was conducted at room temperature (22±2 ℃) and room humidity (55±5 %).

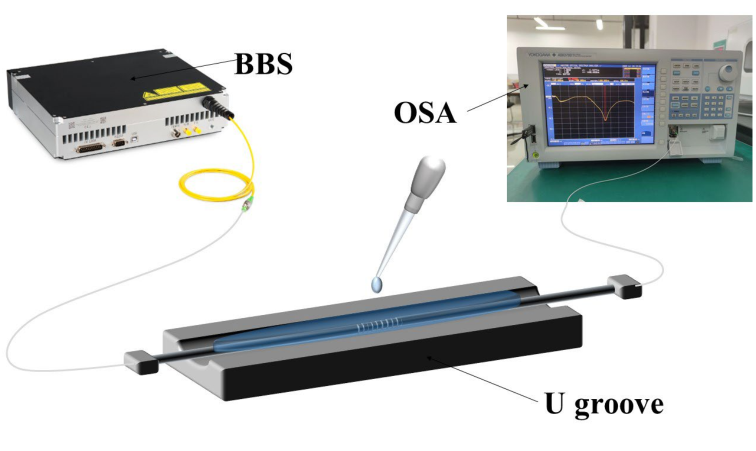

Fig. 3. RI performance detection device.

To obtain optimized sensitivity, we prepared several side-polished LPFGs with different depths (0, 23, 34, and 41 μm) and the same period. Figures 4(a)-(c) show the spectral responses of the LPFG structures with different side-polished depths vs. RI at the range of 1.333. As RI increases, the effective RI of the cladding increases, while the effective RI of the core fundamental mode remains unchanged. Combined with equation (3), the attenuation peaks produced by LPFGs are red-shifted, which may indicate that such LPFGs may have inflection points for a given set of cladding modes [27]. For the resonance wavelength of the positive dispersion point ($d\lambda^{n}_{res}/d\Lambda$ < 0), a red-shift occurs with increasing RI sensitivity. The fitted linear sensitivity is 120.31, 262.74, 391.75, and 466.85 nm/RIU, respectively, corresponding to depths of 0, 23, 34, and 41 μm [Fig. 4(d)]. The deeper the side-polished depth, the stronger the surface evanescent field and the higher the sensor sensitivity. A series of optimal values are obtained at about 41 μm, and the sensitivity is all greater than 423 nm/RIU. However, the side-polished depth should not be too deep, so there will be a balance between structural stability and high sensitivity. At the same time, we studied the reproducibility of the proposed structure. Figure. 4(e) shows that the RI sensitivity of five typical gratings in all LPFGs manufactured with Λ = 550 μm and $d \approx$ 41 μm are 456.47, 423.69, 465.59, 435.14, and 424.85 nm/RIU. It can be seen that this manufacturing technology guarantees the reproduction of high RI sensitivity.

By changing the temperature, the effect of temperature on the RI sensing was further investigated. The effect of temperature on sensor measurements stems from the temperature-dependent response of the sensor itself and the temperature-dependence of the medium. The RI sensitivity of the same sensor was measured at 25, 35, and 45 °C, and assay sensitivity was 466.85, 469.49, and 471.40 nm/RIU, respectively. The results show that the temperature has little effect on the RI sensing within a certain range (Fig. 4(f)).

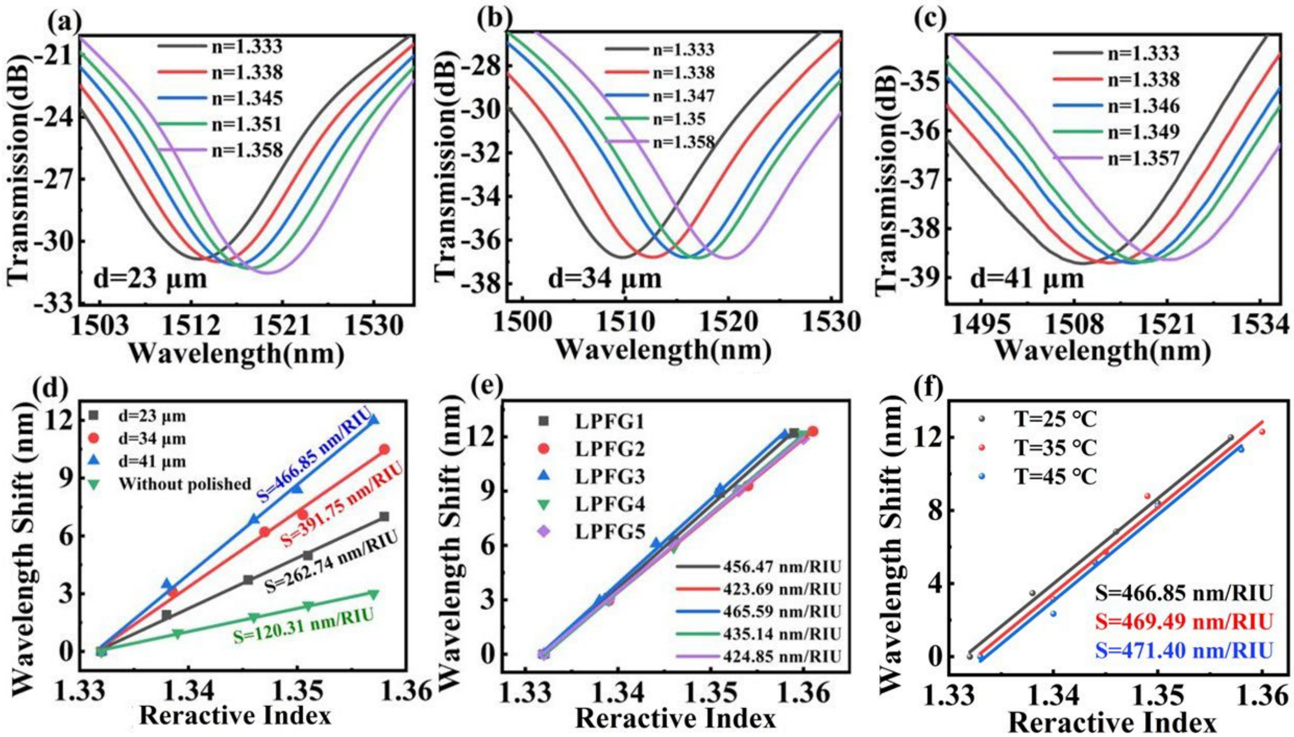

Fig. 4. (a)-(c) The recorded transmission spectra of the LPFG sensor; (d) the RI sensitivity of the LPFG structure with different d; (e) the sensor repeatability was studied by using five sensors in the same test/condition; (f) sensors as a function of RI at 25, 35 and 45 ◦C.

V. Humidity sensing performance

Graphene and its derivatives, as a two-dimensional material to be exfoliated, has been widely researched in the LPFGs sensing applications owing to its superior optical and optoelectronic properties [28-30]. In our trial, the humidity sensing capability of side-polished LPFG is achieved by applying a GO nano-film material coating [31]. GO is a highly oxidized material with various oxygen functional groups on its surface, as shown in Fig. 5 (b). It can change the effective RI by absorbing water molecules. The greater the humidity, the more water molecules will be absorbed, which increases the interlayer distance of GO and causes swelling. When water penetrates the GO, the hydrophilic group can maintain the relative interlayer distance. Therefore, as more water molecules are absorbed, the effective RI of GO decreases [31], [32]. This may change the effective RI of the propagating mode is altered, thereby affecting the wavelength shift.

In this study, the ultrasonically treated GO suspension was coated on the surface of the side-polished LPFG using the dipping method. Then the coated fiber is heated to 70 °C in a drying oven to induce evaporation so that the GO is more firmly placed on the fiber surface shown in Fig. 5(a). Humidity sensing experiments were carried out using side-polished LPFG sensors with GO concentrations of 0.01, 0.05, and 0.1 mg/ml and a fiber period of 550 μm. The sensor was placed in a humidity control box (Xiamen Yeshishi Instrument Co. Ltd. ST-80L), as shown in Fig. 5(c). Change the humidity of the internal environment and analyze the wavelength drift of the sensor when the humidity changes. The temperature (25 °C) and the stress in the test specimen were held constant during the experiment.

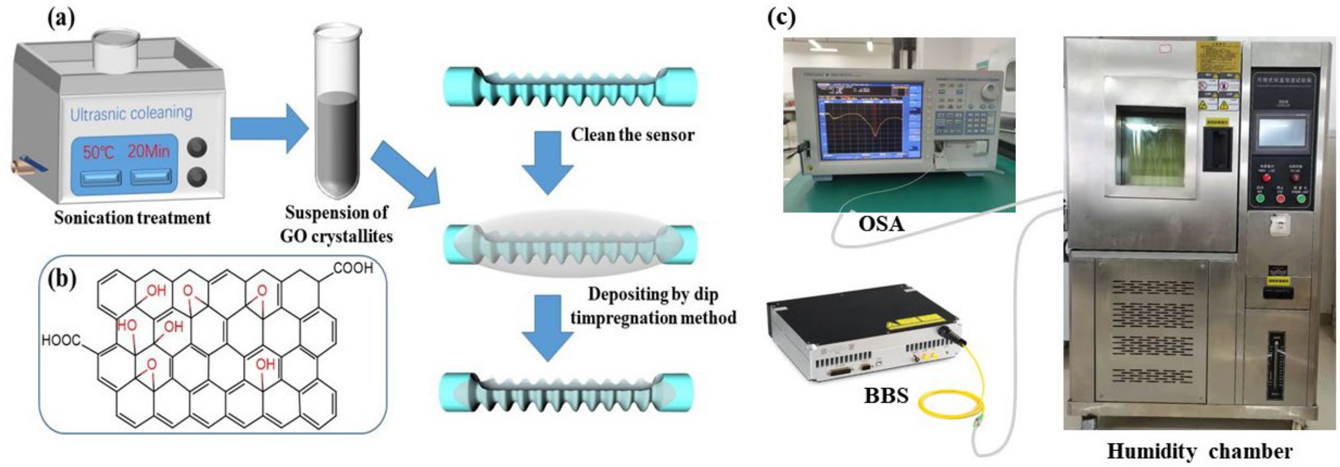

Fig. 5. (a) GO molecular water absorption model; (b) physical map of the humidity detection device; (c) physical map of the humidity detection device.

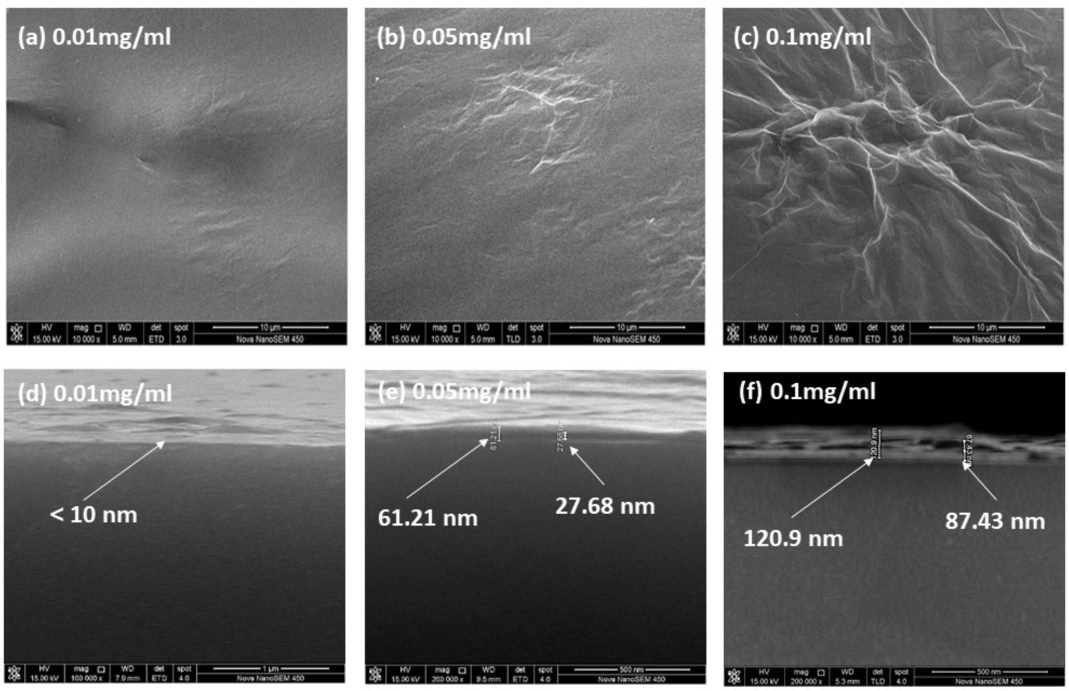

Fig. 6. SEM images of films formed by different concentrations of GO. plan view: (a) 0.01 mg/ml, (b) 0.05 mg/ml and (c) 0.1 mg/ml; cross-sectional view: (d) 0.01 mg/ml, (e) 0.05 mg/ml and (f) 0.1 mg/ml.

Figures 7(a)-(c) shows the RH spectral responses of GO coated with different concentrations in the range of 40%-80%. Combined with equation (3), the attenuation peak of LPFG is blue-shifted with the increase in humidity. This is because as RH grows large, the RI of the GO coating decreases, and the RI of the surrounding environment of the sensor structure decreases, the effective RI of the cladding decreases, while the effective RI of the core fundamental mode remains unchanged. The RH sensitivity of the LPFG coated with three different GO concentrations (0.01, 0.05 and 0.1 mg/ml) is -0.116, -0.193 and -0.133 nm/%RH, respectively (Fig. 7(d)). The coating thicknesses obtained after coating with different concentrations of GO were different, and the surface morphological feature was characterized via SEM, as shown in Fig. 6(a)-(f). The RH sensitivity was maximal within a range of GO concentrations (about 0.05 mg/ml) and much reduced for both thinner (0.01 mg/ml) and thicker (0.1 mg/ml). When it is thinner, the GO layer is difficult to cause changes in RI, when it is thicker, the permeability of water molecules will be blocked [31, 33].

The effect of temperature on humidity sensing was further investigated by changing the temperature. Mainly due to the increase in absolute vapor pressure with increasing temperature, resulting in the adsorption of more water molecules by GO. The RH sensitivity of the same sensor was measured at 25, 35, and 45 °C, and the detection sensitivities were -0.193, -0.223, and -0.269 nm/%RH, respectively. The results showed that the humidity sensitivity increased with the increase in temperature (Fig. 7(e)).

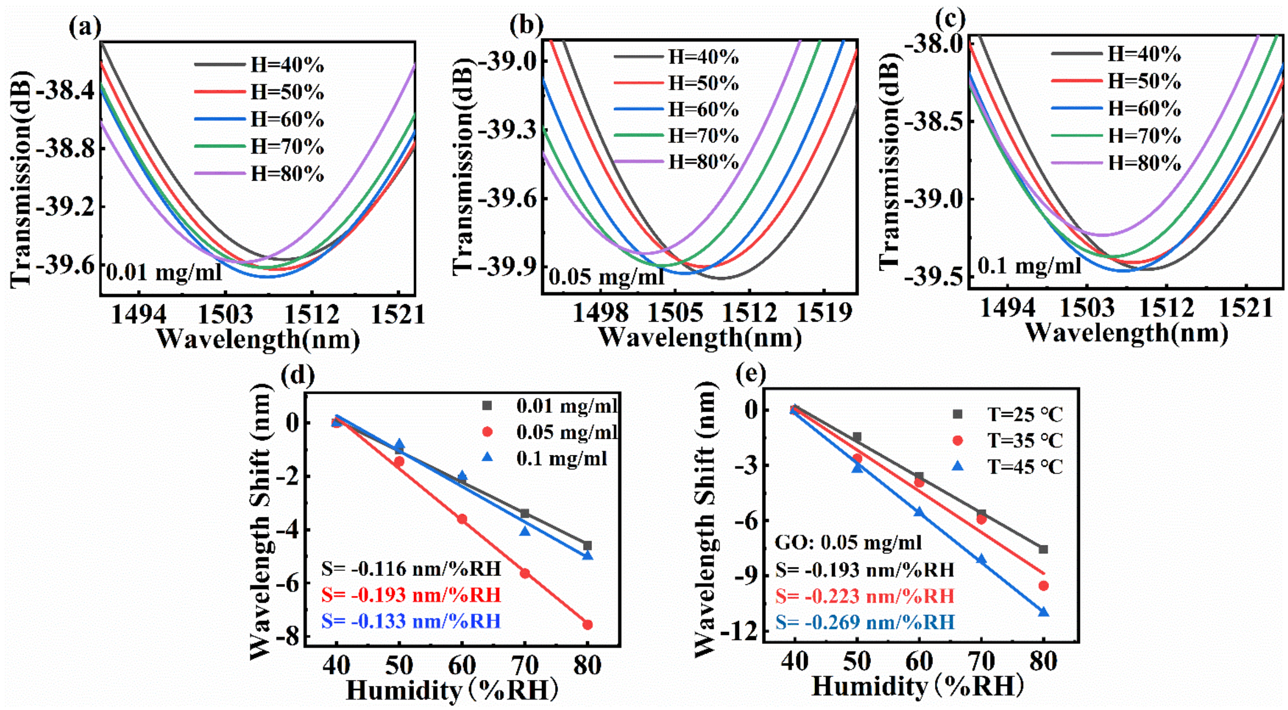

Fig. 7. (a)-(c) The recorded transmission spectra of the LPFG sensor; (d) the RH sensitivity of the LPFG structure with different GO concentrations; (e) sensors as a function of RH at 25, 35, and 45 ◦C.

VI. VECTOR CURVATURE SENSING PERFORMANCE

When the fiber is bent by the external environment, based on the elastic effect of the fiber, the effective RI change of the LPFG will affect the optical path difference between the fiber core mode and the cladding mode, resulting in a wavelength shift. In contrast to traditional LPFG, the side-polished fibers result in asymmetrical light field intensity distribution in the cross-section, thereby realizing curvature vector sense.

The experimental device for curvature characteristics is shown in Fig. 8. The LPFG is fixed between the two translation stages and remains horizontal without applied torsion. Two translation stage was used to vary the distance between the two ends of the translation stage to control the bending curvature. Due to the fiber length being much larger than translating stage stepping length (100 mm >> 0.5 mm). Estimate the bending fiber as a curved arc of a circle, and the curvature was measured by approximating the bending evolution to a circumference function, as previously report described [34]:

$$C = \frac{1}{R} = \frac{2 \cdot d}{(d^2 + L^2)} \tag{4}$$

Where R, d, and L are respectively the radius of curvature, bending displacement, and half of the distance between the two stages.

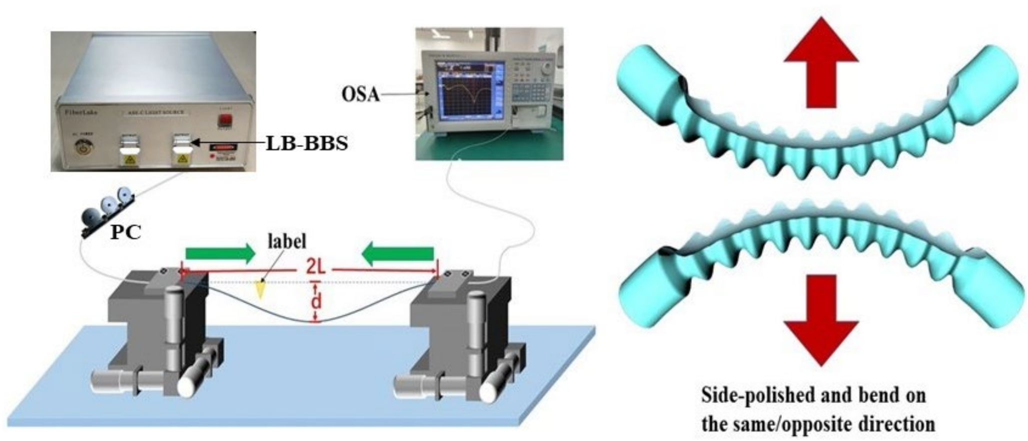

Fig. 8. Experimental setup of curvature sensing.

Figures 9(a), (b), (d), (e), (g) and (h) show the spectral responses for different bending directions. When the LPFG and the side polished surfaces are bent in the same direction, the core is subjected to expansion strain, causing the LPFG peak to shift to longer wavelengths. When the LPFG and side polished surfaces are bent in opposite directions, the core is subjected to compressive strain, causing the LPFG peak to shift to shorter wavelengths. Since the linearity of the linear fit is not high, try to fit a quadratic polynomial equation. The average bending sensitivities for different polarizations (with input light polarization angles of 90°, 45° and 0° degrees selected as representative examples of bending measurements) were calculated to be: 5.03 and -5.9 nm/m^{-1} (Fig. 9(c)), 3.92 and -5.43 nm/m^{-1} (Fig. 9(f)), and 3.05 and -4.37 nm/m^{-1} (Fig. 9(i)), respectively. The experimental results show that the bending sensitivities of the three different input polarized lights of the sensor have certain differences, which may depend on the influence of the input light with different polarization angles on the wavelength and transmission coefficient of the cladding mode during the bending process. These new LPFGs have a well-structured high mechanical strength sufficient to withstand relatively large bending processes (from 0 to 19.67 m^{-1}). The above results show that the proposed side-polished LPFG can achieve vector sensing of curvature direction and radius.

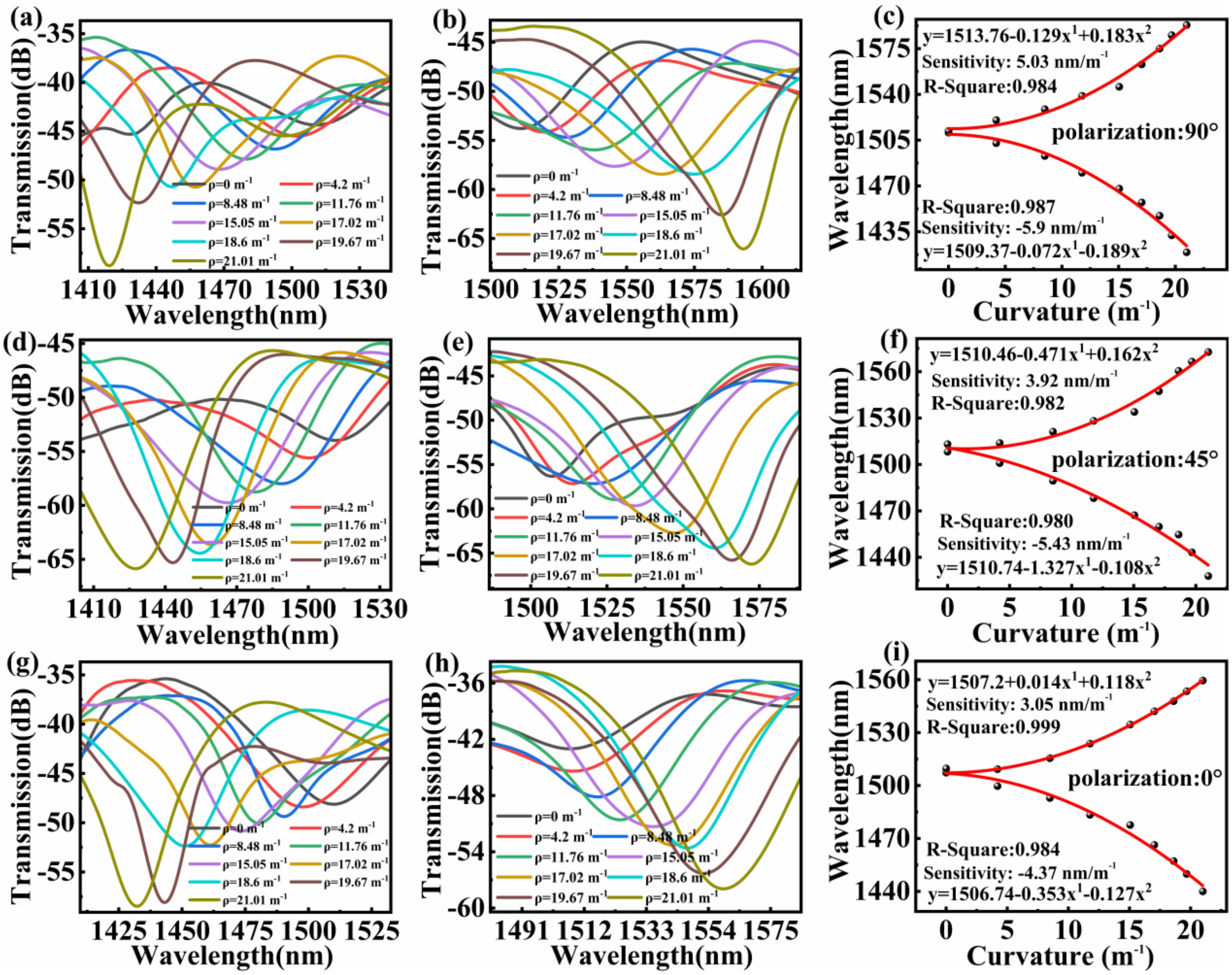

Fig. 9. The influence of the bending radius of LPFG fiber on the spectral response under the boundary conditions of three input light polarization angles: (a), (d), and (g) the same direction bending; (b), (e) and (h) reverse bending; polynomial fitting of dip wavelength shift with curvature: (c) 90°; (f) 45°; (i) 0°.

The proposed sensor is compared with some of the latest methods reported in table I. The table compares the materials, manufacturing methods, and sensing performance (RI, humidity, curvature) of these sensors. In contrast, the sensor reported in this article has superior performance in many aspects, which is a significant result of such a simple and inexpensive sensor manufacturing process.

TABLE I

COMPARISON TABLE

Structure and material	Production Method	RI	Humidity	Curvature	Ref.
LPFG (B/Ge co-doped photosensitive fiber) and GO	Excimer laser and dip-coating	17 - 55 dB/RIU	0.15 dB /%RH	-	[35] (2018)
LPFG (dual side-hole fiber)	EAD	-60.19 nm/RIU	-	21.03 nm/m^{-1} 15.77 dB/m^{-1}	[21] (2018)

Arch-Shaped LPFG (single-mode fiber)	High-frequency CO_2-laser	-	-	22.120 nm/m^{-1} -18.626 nm/m^{-1}	[36] (2018)
LPFG (single-mode fiber) and Polyvinyl alcohol	Etched by HF and coating	-	0.094 nm/%RH	-	[37] (2019)
LPFG	CO_2 laser glass processing	-	-	-42.488 nm/m^{-1}	[38] (2019)
LPFG (pure silica core optical fibers)	EAD	37.94 nm/RIU -98.47 nm/RIU	-	-	[39] (2020)
LPFG (thin-cladding fiber)	EAD	-51.72 nm/RIU	-	-	[19] (2020)
LPFG (single mode fiber) and WS_2	Hydrogen oxygen flame heating and natural evaporation	-	0.0373 nm/%RH	-	[40] (2021)
Sied-polished LPFG (single-mode fiber) and GO	Sied-polished, EAD, and dip-coating	466.85 nm/RIU	0.193 nm/%RH	5.03 nm/m^{-1} -5.9 nm/m^{-1}	This work

VII. Conclusion

The characteristics of the LPFG sensor based on side-polished have been studied in this article experimentally. The RI characteristics of the LPFG sensor show that the side-polished can effectively enhance the evanescent field of LPFG and significantly increase sensitivity. The greater the depth, the more pronounced the increased sensitivity. And by coating a layer of GO film on the sensor surface, high-sensitivity humidity sensing is realized. Moreover, the break of symmetry of the optical fiber structure, and the vector curvature measurement is implemented. The experimental results show that the use of side-polished LPFG sensors will lead to better detection performance, and may provide better experimental design and potential applications for the preparation of LPFG sensors by EDA technology.

References

[1] V. Arya, D. W. Sherrer, A. Wang, R. O. Claus and M. Jones, “Application of thin-film optical filters to the temperature compensation of optical fiber grating-based devices,” *IEEE Trans. Instrum. Meas.*, vol. 46, no. 5, pp. 1173-1177, 1997.

[2] S. Aristilde, C. Cordeiro and J. H. Osório, “Gasoline Quality Sensor Based on Tilted Fiber Bragg Gratings,” *Photonics*, vol. 6, no. 2, pp. 51, 2019.

[3] J. Sun, C. C. Chan, X. Y. Dong, and P. Shum, “Application of anartificial neural network for simultaneous measurement of temperature and strain by using a photonic crystal fiber long-period grating,” *Meas. Sci. Technol.*, vol. 18, no. 9, pp. 2943 – 2948, 2007.

[4] Z. C. Zhuo and B. S. Ham, “A temperature-insensitive strain sensor using a fiber Bragg grating,” *Opt. Fiber Technol.*, vol. 15, no. 5-6, pp. 442-444, 2009.

[5] G. R. C. Possetti, L. C. Cocco, C. I. Yamamoto, L. V. R. de Arruda, R. Falate, M. Muller and J. L. Fabris, “Application of a long-period fibre grating-based transducer in the fuel industry,” *Meas. Sci. Technol.*, vol. 20, no. 3, pp. 034012, 2009.

[6] T. Wieduwilt, Brückner, Sven and H. Bartelt, “High force measurement sensitivity with fiber Bragg gratings fabricated in uniform-waist fiber tapers” *Meas. Sci. Technol.*, vol. 22, no. 7, pp. 75201-75206(6), 2011.

[7] F. Barino, F. S. Delgado, M. A. Jucá, T. V. N. Coelho and A. B. D. Santos, “Comparison of Regression Methods for Transverse Load Sensor based on Optical Fiber Long-Period Grating,” *Measurement*, vol. 146, no. 6, 2019.

[8] Q. H. Hu, P. R. Wang, M. Wang and Z. F. Wang, “Fabrication of superimposed fiber Bragg gratings and applications in fiber laser oscillators - ScienceDirect,” *Optik*, vol. 214, pp. 164583, 2020.

[9] K. Dominik, S. B. Gabriela, M. Pawel and U. Waclaw, “Microstructured polymer optical fiber for long period gratings fabrication using an ultraviolet laser beam,” *Opt. Lett.*, vol. 39, no. 8, pp. 2242-5, 2014.

[10] F. Hindle, E. Fertein, C. Przygodzki, F. Durr, L. Paccou, R. Bocquet, P. Niay, H. G. Limberger and M. Douay, “Inscription of long-period gratings in pure silica and Germano-silicate fiber cores by femtosecond laser irradiation,” *IEEE Photonics Technol. Lett.*, vol. 16, no. 8, pp. 1861-1863, 2004.

[11] D. Noordegraaf, L. Scolari, J. Lægsgaard, L. Rindorf and T. T. Alkeskjold, “Electrically and mechanically induced long period gratings in liquid crystal photonic bandgap fibers,” *Opt. Express*, vol. 15, no. 13, pp. 7901-12, 2007.

[12] J. Yan, Q. Li, C. H. Lin, E. Lyons, I. Tomov and H. P. Lee, “A novel strain-induced thermally tuned long-period fiber grating fabricated on a periodic corrugated silicon fixture,” *IEEE Photonics Technol. Lett.*, vol. 14, no. 7, pp. 941-943, 2002.

[13] GRANT and A. ROBERTS, “Long Period Gratings in Multimode Fiber Fabricated with High-Energy Ion Implantation,” *Fiber Integr. Opt.*, vol. 22, no. 4, pp. 225-237, 2003.

[14] R. Kritzinger, D. Schmieder and A. Booysen, “Azimuthally symmetric long period fibre grating fabrication with a TEM_{01}*-mode CO_2 laser,” *Meas. Sci. Technol.*, vol. 20, no. 3, pp. 034004, 2009.

[15] X. R. Jin, C. P. Lu, J. Y. Lin, X. D. Chen, X. Y. Li, Z. H. Xiang, X. H. Yang, C. G. Tong, Y. X. Yan, T. Geng, W. M. Sun and L. B. Yuan, “A strain sensor with low temperature crosstalk based on re-modulation of D-shaped LPFG – Science Direct,” *Measurement*, vol. 177, pp. 109300, 2021.

[16] G. Yin, Y. Wang, C. Liao, J. Zhou, X. Zhong, G. Wang, B. Sun and J. He, “Long Period Fiber Gratings Inscribed by Periodically Tapering a Fiber,” *IEEE Photonics Technol. Lett.*, vol. 26, no. 7, pp. 698-701, 2014.

[17] G. Yin, Y. Wang, C. Liao, B. Sun, Y. Liu, S. Liu, Q. Wang, K. Yang, J. Tang and X. Zhong, “Simultaneous refractive index and temperature measurement with LPFG and liquid-filled PCF,” *IEEE Photon. Technol. Lett.*, vol. 27, no. 4, pp. 375–378, 2015.

[18] C. Du, Y. Zhao, Q. Wang and F. Xia, “Sensitivity-optimized long-period fiber gratings for refractive index and temperature sensing,” *Instrum. Sci. Technol.*, vol. 46, no. 4, pp. 435-449, 2017.

[19] M. Luo and Q. Wang, “Fabrication and sensing characteristics of arc-induced long-period fiber gratings based on thin-cladding fiber,” *Alexandria Eng. J.*, vol. 59, no. 5, pp. 3681-3686, 2020.

[20] L. Coelho, D. Viegas, J. L. Santos and J. MMMde Almeida, “Enhanced refractive index sensing characteristics of optical fibre long period grating coated with titanium dioxide thin films,” *Sens. Actuators, B*, vol. 202, pp. 929-934, 2014.

[21] Y. Zhou, Z. T. Gu and Q. Ling, “Sensing Characteristics of Uncoated Double Cladding Long-period Fiber Grating Based on Mode Transition and Dual-peak Resonance” *Curr. Opt. Photonics*, vol. 5, no. 3, pp. 243-249, 2021.

[22] M. Lai, Y. Zhang, Z. Li, W. Zhang, H. Gao, L. Ma, H. Ma and T. Yan, “High-sensitivity bending vector sensor based on γ-shaped long-period fiber grating” *Opt. Laser Technol.*, vol. 142, pp. 107255, 2021.

[23] O. Y. Yang, H. Y. Guo, X. W. Ouyang and X. F. Xu, “Highly Sensitive Two-axis Bending Sensor Based on Arc-induced Long Period Fiber Grating in Dual Side Hole Fiber,” *IEEE Photonics J.*, vol. 10, no. 1, 2017.

[24] W. T. MacDougall, S. Pilevar, W. C. Haggans and A. M. Jackson, “Generalized expression for the growth of long period gratings,” *IEEE Photonics Technol. Lett.*, vol. 10, no. 10, pp. 1449–1451, 1998.

[25] H. Ahmad, I. S. Amiri, A. Z. Zulkifli, H. Hassan, R. Safaei and K. Thambiratnam, “Stable dual-wavelength erbium-doped fiber laser using novel fabricated side-polished arc-shaped fiber with deposited ZnO nanoparticles,” *Chin. Opt. Lett.*, vol. 15, no. 1, pp. 011403, 2017.
[26] X. Yi, X. Dong, J. Yuan, L. Yi, S. Jin and S. Zhang, “Sensing Characteristics of Side-Hole Fiber-Based Long-Period Grating,” *Adv. Mater. Sci. Eng.*, vol. 2013, no. 11, pp. 2070-2074, 2013.
[27] X. Shu, Z. Lin, I. Bennion, “Sensitivity characteristics near the dispersion turning points of long-period fiber gratings in B/Ge codoped fiber,” *Opt. Lett.*, vol. 26, no. 22, pp. 1755, 2001.
[28] R. Wang, X. Kang, D. Kong, M. Jiang, Z. Ren, B. Hu and Z He, “Highly sensitive metal ion sensing by graphene oxide functionalized micro-tapered long-period fiber grating,” *Analyst*, vol. 13, pp. 147, 2022.
[29] R. Wang, W. U. Hao, Q. I. Mei, J. Han and Z. Ren, “Bovine Serum Albumin Detection by Graphene Oxide Coated Long-Period Fiber Grating,” *Photonic Sens.*, vol. 12, no. 3, pp. 1-10, 2022.
[30] L. Dong, K. Zhao, J. Wu, G. Deng and C. Tang, “A vapochromic dye/graphene coated long-period fiber grating for benzene vapor sensing,” *Mater. Chem. Front.*, vol. 6, no. 17, pp. 2438-2446, 2022.
[31] Y. Q. Wang, C. Y. Shen, W. M. Lou, F. Y. Shentu, C. Zhong, X. Y. Dong, and L. M. Tong, “Fiber optic relative humidity sensor based on the tilted _ber Bragg grating coated with graphene oxide,” *Appl. Phys. Lett.*, vol. 109, no. 3, 2016.
[32] N. Sahoo, Z. Sun, K. Zhou, X. Chen, Y. Tanl and L. Zhang, “Graphene-oxide coated LPGs for humidity sensing applications,” *Micro-Structured and Specialty Optical Fibres VI*, vol. 11355, 2020.
[33] Y. Wang, C. Shen, W. Lou and F. Shentu, “Polarization-dependent humidity sensor based on an in-fiber Mach–Zehnder interferometer coatedwith graphene oxide,” *Sens. Actuators, B*, vol. 234, pp. 503-509, 2016.
[34] H. P. Gong, H. F. Song, S. L. Zhang and Y. Jin, “Curvature sensor based on hollow-core photonic crystal fiber sagnac interferometer,” *IEEE Sens. J.*, vol. 14, no. 3, pp. 777-780, 2014.
[35] K. P. W. Dissanayake, W. Wu, H Nguyen, T. Sun and K. T. V. Grattan, “Graphene-Oxide-Coated Long-Period Grating-Based Fiber Optic Sensor for Relative Humidity and External Refractive Index,” *J. Lightwave Technol.*, vol. 36, no. 4, pp. 1145-1151, 2018.
[36] Y. X. Zhang, W. G. Zhang, Y. S. Zhang, S. Wang, L. J. Bie, L. X. Kong, P. C. Geng and T. Y. Yan, “Bending Vector Sensing Based on Arch-Shaped Long-Period Fiber Grating,” *IEEE Sens. J.*, vol. 18, no. 8, pp. 3125-3130, 2018.
[37] Y. F. Qi, C. Jia, L. Tang, X. Zhang, C. B. Gong, Y. Y. Liu and X. Q. Liu, “Research on temperature and humidity sensing characteristics of cascaded LPFG-FBG - ScienceDirect,” *Optik*, vol. 188, pp. 19-26, 2019.
[38] J. A. Martin-Vela, J. M. Sierra-Hernandez, A. Martinez-Rios, J. M. Estudillo-Ayala and D. Jauregui-Vazquez, “Curvature Sensing Setup Based on a Fiber Laser and a Long-Period Fiber Grating,” *IEEE Photonics Technol. Lett.*, vol. 31, no. 15, pp. 1265-1268, 2019.
[39] A. Srivastava, F. Esposito, A. Iadicicco and S. Campopiano, “Long Period Fiber Grating Sensors Fabricated by Electric Arc Discharge Technique Sensors and Microsystems,” *Lecture Notes in Electrical Engineering*, vol. 629, pp. 395-402, 2020.
[40] J. Wang, “Surface plasmon resonance humidity sensor based on twisted long period fiber grating coated with tungsten disulfide film,” *Optik*, vol. 236, pp. 166616, 2021.

Hou-Chang Li is a graduate student with the School of Measuring and Optical Engineering, Nanchang Hangkong University. Her research interest is fiber optic sensing.

Juan Liu received her Ph.D. degree from Beijing Normal University, China. She is a lecture with Key Laboratory of Nondestructive Test (Ministry of Education) of Nanchang Hangkong University, China. Her main research interest is fiber optic sensing.

Xing-Dao He was born in Jingan, China, in 1963. He received the Ph.D. degree in optics from Beijing Normal University, Beijing, China, in 2005. He is currently a Professor with the Key Laboratory of Nondestructive Test (Ministry of Education), Nanchang Hangkong University, China. His current research interests include light scattering spectroscopy, optical holography, and information processing.

Jinhui Yuan received the Ph.D. degree in physical electronics from Beijing University of Posts and Telecommunications (BUPT), Beijing, China, in 2011. He is currently a Professor at the Department of computer and communication engineering, University of Science and Technology Beijing (USTB). He was selected as a Hong Kong Scholar at the Photonics Research Centre, Department of Electronic and Information Engineering, The Hong Kong Polytechnic University, in 2013. His current research interests include photonic crystal fibers, silicon waveguide, and optical fiber devices. He is the Senior Members of the IEEE and OSA. He has published over 200 papers in the academic journals and conferences.

Qiang Wu received the B.S. and Ph.D. degrees from Beijing Normal University and Beijing University of Posts and Telecommunications, Beijing, China, in 1996 and 2004, respectively. From 2004 to 2006, he worked as a Senior Research Associate in City University of Hong Kong. From 2006 to 2008, he took up a research associate post in Heriot-Watt University, Edinburgh, U.K. From 2008 to 2014, he worked as a Stokes Lecturer at Photonics Research Centre, Dublin Institute of Technology, Ireland. He is an Associate Professor / Reader with Faculty of Engineering and Environment, Northumbria University, Newcastle Upon Tyne, United Kingdom. His research interests include optical fiber interferometers for novel fiber optical couplers and sensors, nanofiber, microsphere sensors for bio-chemical sensing, the design and fabrication of fiber Bragg grating devices and their applications for sensing, nonlinear fibre optics, surface plasmon resonant and surface acoustic wave sensors. He has over 200 publications in the area of photonics and holds 3 invention patents. He is an Editorial Board Member of Scientific Reports, an Associate Editor for IEEE Sensors Journal and an Academic Editor for Journal of Sensors.

Bin Liu (Member, IEEE) received the B.S. and Ph.D. degrees from Sun Yat-sen University, China. Dr. Liu is an Associate Professor with the Key Laboratory of Opto-Electronic Information Science and Technology of Jiangxi Province, Nanchang Hangkong University, China. He has over 80 publications in the area of photonics and holds 10 invention patents. His current research interests include optical fiber interferometer and the application for sensing, fiber bio-chemical sensors, optical micro-cavity and the application for sensing, surface plasmon resonant, Design and application of micro-nano photonic devices, optical nonlinearity and optical soliton, FBG sensing and distributed fiber sensing.